

# Epistemic Uncertainty for NGA-West2 Models

Linda Al Atik<sup>a)</sup> and Robert R. Youngs<sup>b)</sup> M.EERI

The development of the NGA-West2 ground motion prediction equations (GMPEs) is a collaborative effort with many interactions and exchange of ideas among the developers. The NGA-West2 developers indicate that additional epistemic uncertainty needs to be incorporated into the median ground motion estimation from each of the five NGA-West2 GMPEs in order to more fully represent an appropriate level of epistemic uncertainty. A proposed minimum additional epistemic uncertainty is evaluated based on statistical estimates of the uncertainty in the median predictions of each GMPE. The proposed additional epistemic uncertainty model is distance-independent but depends on magnitude, style of faulting (SOF), and spectral period. The epistemic uncertainty in the median predictions from each GMPE is then modeled using a three-point discrete approximation to a normal distribution. [DOI: 10.1193/062813EQS173M]

## INTRODUCTION

It is common practice in probabilistic seismic hazard analysis (PSHA) to represent the epistemic uncertainty in estimating earthquake ground motions by a weighted set of the available ground motion prediction equations (GMPEs) considered appropriate. The underlying assumption of this approach is that the set of models, which typically have been developed more or less independently by various researchers, represents the range of technically defensible interpretations for modeling strong ground motions. However, the original set of NGA GMPEs described in [Abrahamson et al. \(2008\)](#); hereafter, NGA-West1) and the updated set of NGA-West2 GMPEs presented in this volume represent a somewhat unique situation. Although the five NGA-West2 GMPEs were developed using different functional forms and different subsets of the NGA-West2 ground motion database, there was a great deal of collaboration among the development teams and the use of common sets of statistical analyses and simulations to constrain parts of the models. Furthermore, the focus of the five development teams was on developing a good representation of the expected level of ground motions as a function of the chosen predictor variables, rather than “capturing the center, body, and range of technically defensible interpretations,” as would have been the case if the overall project was conducted following the guidance provided in NUREG-2117 ([USNRC 2012](#), p. 34). Recognizing this, the NGA developers recommended that additional epistemic uncertainty be incorporated into the median ground motion estimation when applying the NGA-West2 model set.

---

<sup>a)</sup> Linda Alatik Consulting, San Francisco, CA 94110

<sup>b)</sup> AMEC Environment & Infrastructure Inc., 2101 Webster St., 12<sup>th</sup> Floor, Oakland, CA 94612

In the first major application of the NGA-West1 models, [Petersen et al. \(2008\)](#) incorporated additional epistemic uncertainty to account for “data limitations (especially for large earthquakes) and the considerable interaction between modelers” (p. 38). [Petersen et al. \(2008\)](#) assumed a 90% confidence interval of 0.4 natural log units in median ground motions for earthquakes of  $M \geq 7$  at distances  $\leq 10$  km. They then used the relative number of earthquakes contributing data to various magnitude and distance intervals to define the levels of uncertainty for other magnitude and distance ranges.

The NGA-West1 GMPEs were derived for the most part using regression analyses of empirical ground motion data. As a result, statistical techniques are available to directly quantify the uncertainty in the mean estimates derived from regression models without the need to assume an uncertainty level. [BC Hydro \(2012\)](#) used this approach to quantify the uncertainty in the median ground motion predictions obtained using the [Chiou and Youngs \(2008\)](#) model. BC Hydro then represented the epistemic uncertainty in median ground motion estimation by using an equally weight set of the 2008 NGA GMPEs and applied the uncertainty in the median predictions for the [Chiou and Youngs \(2008\)](#) GMPE to the other NGA-West1 GMPEs.

In the following, we apply the statistical approach used by [BC Hydro \(2012\)](#) to estimate the minimum additional epistemic uncertainty to be added to the NGA-West2 GMPE set. We first evaluate the model-to-model differences in the median predictions of the five models: [Abrahamson et al. \(2014; ASK14\)](#), [Boore et al. \(2014; BSSA14\)](#), [Campbell and Bozorgnia \(2014; CB14\)](#), [Chiou and Youngs \(2014; CY14\)](#), and [Idriss \(2014; Id14\)](#). The uncertainty in the median predictions from each GMPE is then calculated statistically based on the model fit and the data distribution while taking into account the imposed model constraints. The model-to-model differences are compared to the uncertainty in the median prediction from each GMPE and an epistemic uncertainty model is proposed for use with the set of five equally weighted NGA-West2 models.

## APPROACH

The model-to-model variability and statistical uncertainty in median predictions from the set of five NGA-West2 models are evaluated using the rupture geometries shown in [Figure 1](#). The analysis is performed for  $V_{S30}$  of 760 m/s. The selection of fault dip angles was based on the approximate average values for the earthquakes in the NGA-West2 database. The model-to-model variability in the median predictions of the NGA-West2 GMPEs is estimated in terms of the standard deviation in the natural logarithm of the predicted median ground motion,  $\sigma_{\mu \ln(SA)}$ , as shown in [Equation 1](#):

$$\sigma_{\mu \ln(psa)} = \sqrt{\frac{\sum_i w_i [\mu_{\ln(psa)_i} - \overline{\mu_{\ln(psa)}}]^2}{\sum_i w_i}} \quad (1)$$

with

$$\overline{\mu_{\ln(psa)}} = \frac{\sum_i w_i \mu_{\ln(psa)_i}}{\sum_i w_i} \quad (2)$$

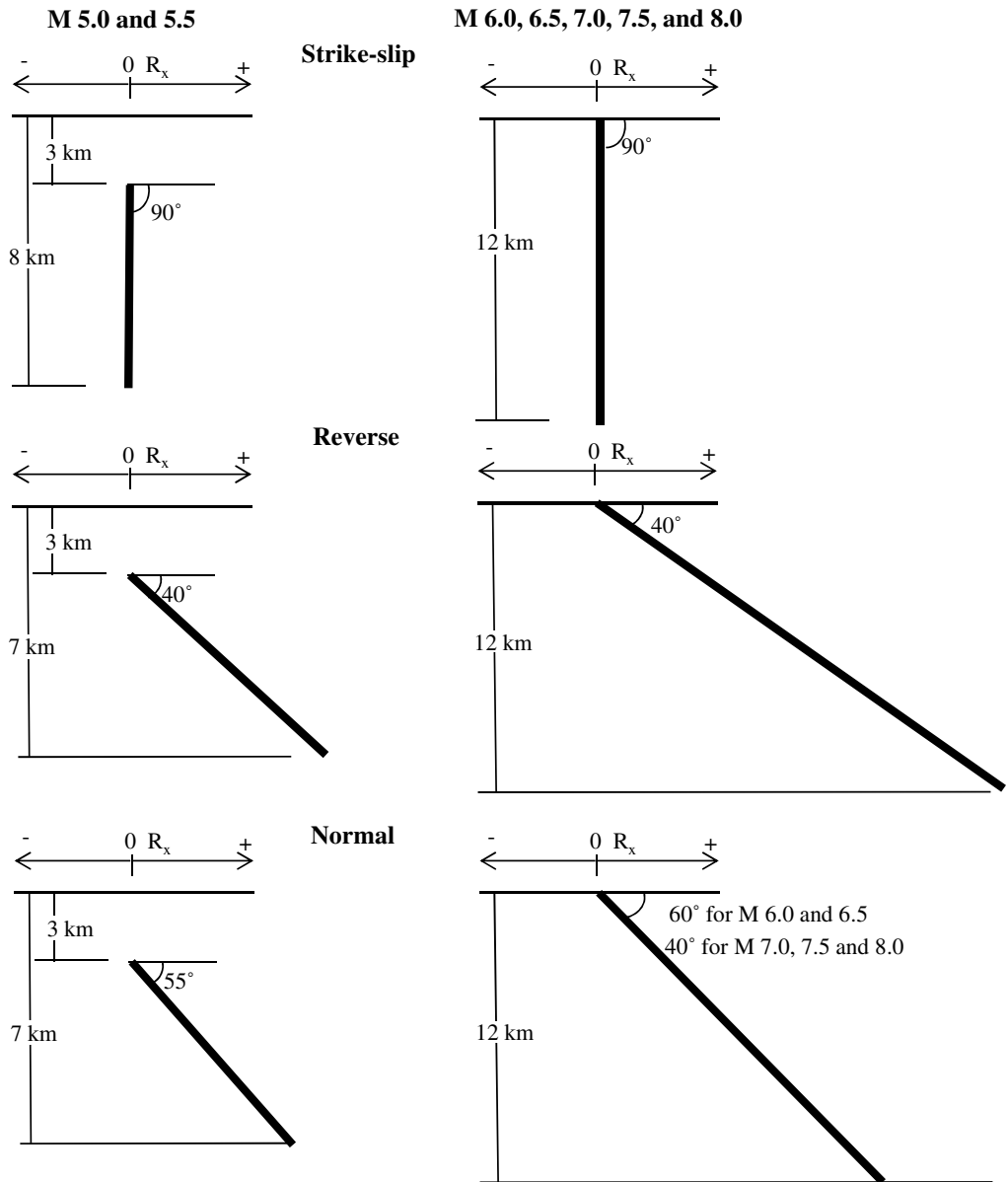


**Figure 1.** Rupture geometries used for evaluating the epistemic uncertainty for NGA-West2 GMPEs.

where  $\mu_{\ln(psa)_i}$  is the natural logarithm of the median ground motion predicted by the  $i^{\text{th}}$  GMPE, and  $w_i$  is the probability weight assigned for the  $i^{\text{th}}$  model. The model-to-model variability is evaluated for a range of horizontal distances from the top of rupture measured perpendicular to fault strike ( $R_x$ ) of 1 km to 300 km on the hanging wall side.

The uncertainty in the median prediction from each of the five NGA-West2 models (within-model uncertainty) is evaluated based on the statistics of the model fit and the empirical data distribution used for the model. This approach assesses how well the empirical data constrains each model while incorporating the additional constraints imposed on the model.

The NGA-West2 GMPEs are developed through mixed-effects regression models of the general form (e.g., [Abrahamson and Youngs 1992](#)):

$$\ln(PSA_{ij}) = f(\mathbf{x}_{ij}, \mathbf{c}) + \eta_i + \varepsilon_{ij} \quad (3)$$

where  $PSA_{ij}$  is the peak pseudo-spectral acceleration at a given spectral period for the  $j^{\text{th}}$  recording of the  $i^{\text{th}}$  earthquake,  $\mathbf{x}_{ij}$  is the vector of predictor variables,  $\mathbf{c}$  is the vector of model coefficients,  $\eta_i$  is the event term for the  $i^{\text{th}}$  earthquake, and  $\varepsilon_{ij}$  is a random error term representing the variability of the  $j^{\text{th}}$  recording about the average motion for the  $i^{\text{th}}$  earthquake (intra-event variability). The coefficients  $\mathbf{c}$  are found by maximizing the log-likelihood function given by [Searle \(1971\)](#):

$$LL = \frac{1}{2} \ln |\mathbf{V}| + \frac{1}{2} [\mathbf{y} - f(\mathbf{x}, \mathbf{c})]^T \mathbf{V}^{-1} [\mathbf{y} - f(\mathbf{x}, \mathbf{c})] \quad (4)$$

where  $\mathbf{y} = \ln(PSA)$ , and  $\mathbf{V}$  is the block diagonal variance matrix of the data.

Using a Taylor series expansion, [Seber and Wild \(1989\)](#) show that the asymptotic variance of a future prediction of a nonlinear model at location  $\mathbf{x}_0$  is given by:

$$\text{var}[\mathbf{y}]_{\mathbf{x}_0} = \sigma^2 + \sigma^2 \mathbf{f}_0^T [\mathbf{F}^T \mathbf{F}]^{-1} \mathbf{f}_0 \quad (5)$$

in which  $\mathbf{F}$  is the gradient of the predictive function with respect to the coefficients evaluated at the data points  $\mathbf{x}_i$  used to develop the model,

$$\mathbf{F} = \left. \frac{\partial f(\mathbf{x}, \mathbf{c})}{\partial \mathbf{c}} \right|_{\mathbf{x}_i} \quad (6)$$

and  $\mathbf{f}_0$  is the gradient of the predictive function evaluated at the new location  $\mathbf{x}_0$ :

$$\mathbf{f}_0 = \left. \frac{\partial f(\mathbf{x}, \mathbf{c})}{\partial \mathbf{c}} \right|_{\mathbf{x}_0}. \quad (7)$$

The first term on the right of Equation 5 is the variance of the data about the mean prediction and the second term is the variance of the mean prediction, with the term  $\sigma^2 [\mathbf{F}^T \mathbf{F}]^{-1}$  representing the linearized asymptotic variance matrix for the coefficients  $\mathbf{c}$ .

Equation 5 is based on a model in which the data have a homoscedastic error structure with variance matrix  $\sigma^2 \mathbf{I}$ . As shown in [Searle \(1971\)](#), the variance matrix for the coefficients  $\mathbf{c}$  in a mixed-effects model is given by  $[\mathbf{F}^T \mathbf{V}^{-1} \mathbf{F}]^{-1}$ . Substituting this term into Equation 5 and retaining only the portion that gives the variance of the mean prediction yields the expression:

**Table 1.** Fixed coefficients in NGA-West2 models

Model	Fixed coefficients
ASK14	$V_{lin}, b, n, c, M_1, M_2$
BSSA14	$M_h, M_{ref}, R_{ref}, V_{ref}, V_c, e_0$
CB14	$k_1, k_2, k_3, n, c, a_2, h_1, h_2, h_3, h_4, h_5, h_6$
CY14	$c_2, c_4, c_{4a}, c_{RB}, c_9, c_{9a}, c_{9b}, \phi_4, \phi_6, \phi_{6JP}$
Id14	None

$$\text{var}[\bar{y}]_{\mathbf{x}_0} = \sigma_{\ln(PSA)}^2 \Big|_{\mathbf{x}_0} = \mathbf{f}_0^T [\mathbf{F}^T \mathbf{V}^{-1} \mathbf{F}]^{-1} \mathbf{f}_0. \quad (8)$$

Equation 8 is used to assess the uncertainty in the median (mean  $\ln[PSA]$ ) prediction from each of the five NGA-West2 models for the scenarios shown in Figure 1. The values of the predictor variables  $\mathbf{x}_0$  for the scenarios are defined for sites on the hanging wall in the distance range,  $R_x$ , of 1 to 300 km, with  $V_{S30}$  equal to 760 m/s. The set of coefficients that are considered fixed (constrained) in each model are listed in Table 1. These coefficients were not determined from the regression analysis but pre-selected by the model developers based on additional considerations, such as physical models or numerical simulations.

## RESULTS

Figures 2, 3, and 4 show the computed within-model uncertainty in median prediction of each of the five NGA-West2 models for the strike-slip (S), reverse (R), and normal faulting (N) earthquake rupture scenarios, respectively, defined in Figure 1. Each figure shows the results for peak ground acceleration (PGA) and 1 s pseudo-spectral acceleration (PSA) for magnitude  $M$  5.5,  $M$  6.5, and  $M$  7.5 earthquakes. The results indicate that the asymptotic standard error in median ground motion is larger for normal faulting earthquakes than for strike-slip and reverse-faulting earthquakes. This is primarily due to the smaller amount of data from normal faulting earthquakes in the NGA-West2 database compared to that from reverse and strike-slip earthquakes. Similarly, the within-model uncertainty is larger for the  $M$  7.5 scenarios than for the  $M$  6.5 and  $M$  5.5 scenarios due to the limited amount of data from earthquakes with  $M$  7 to  $M$  8 in the NGA-West2 database. The differences in within-model uncertainty among the five GMPEs for the same scenario reflects differences in the amount of data used by each development team, differences in functional form, and model constraints. All the models show some distance dependence in the within-model uncertainty, with a general increase in the uncertainty at distances larger than 200 km. CY14 shows the largest within-model uncertainty for dip-slip scenarios.

Also shown on each plot of Figures 2 through 4 is the model-to-model variability computed using Equations 1 and 2 with equal weights assigned to the five GMPEs. These results show that the model-to-model variability among the five GMPEs is generally larger than the asymptotic standard errors in the median predictions for the individual GMPEs. The model-to-model variability is generally largest for sites located over the hanging wall of dipping ruptures and at larger distances.

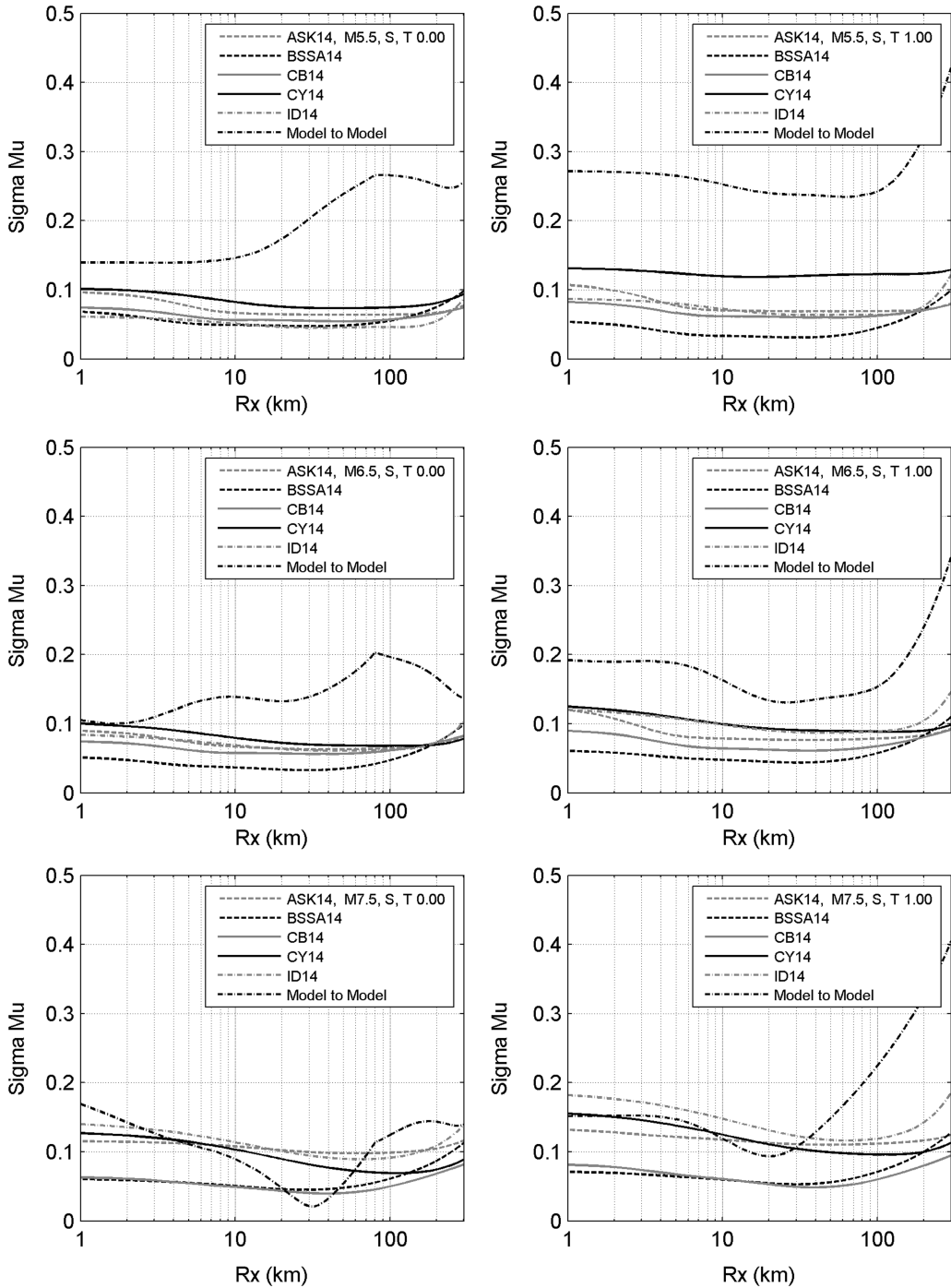


**Figure 2.** Asymptotic standard errors and model-to-model variability in median  $\ln(\text{PSA})$  for the five NGA-West2 models for the strike-slip (S) rupture scenarios shown in Figure 1. Results are shown for PGA (left column) and 1.0 s PSA (right column) for  $M$  5.5 (top row),  $M$  6.5 (middle row), and  $M$  7.5 (bottom row) earthquakes.

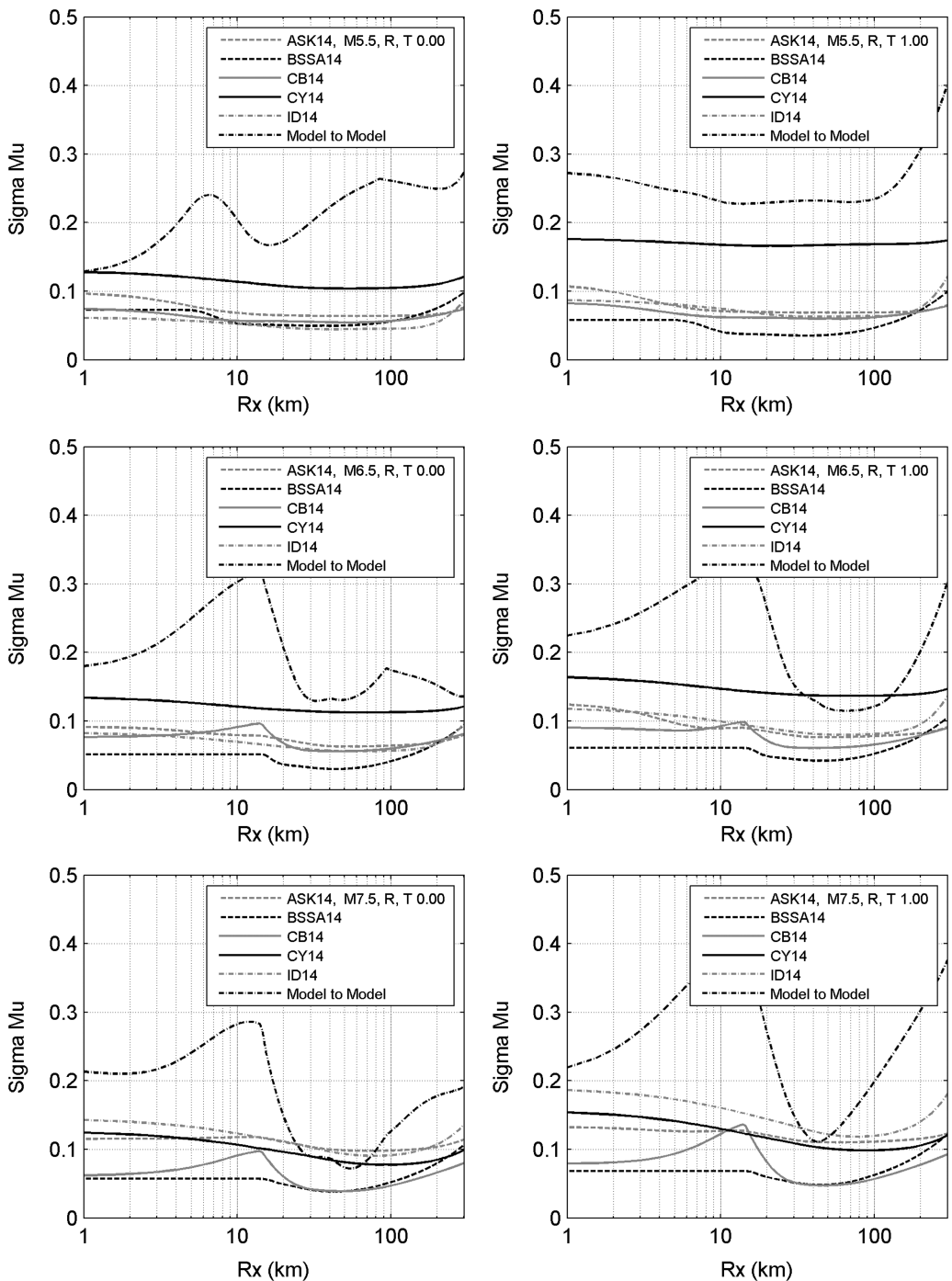


**Figure 3.** Asymptotic standard errors and model-to-model variability in median  $\ln(\text{PSA})$  for the five NGA-West2 models for the reverse (R) rupture scenarios shown in Figure 1. Results are shown for PGA (left column) and 1.0 s PSA (right column) for  $M$  5.5 (top row),  $M$  6.5 (middle row), and  $M$  7.5 (bottom row) earthquakes.

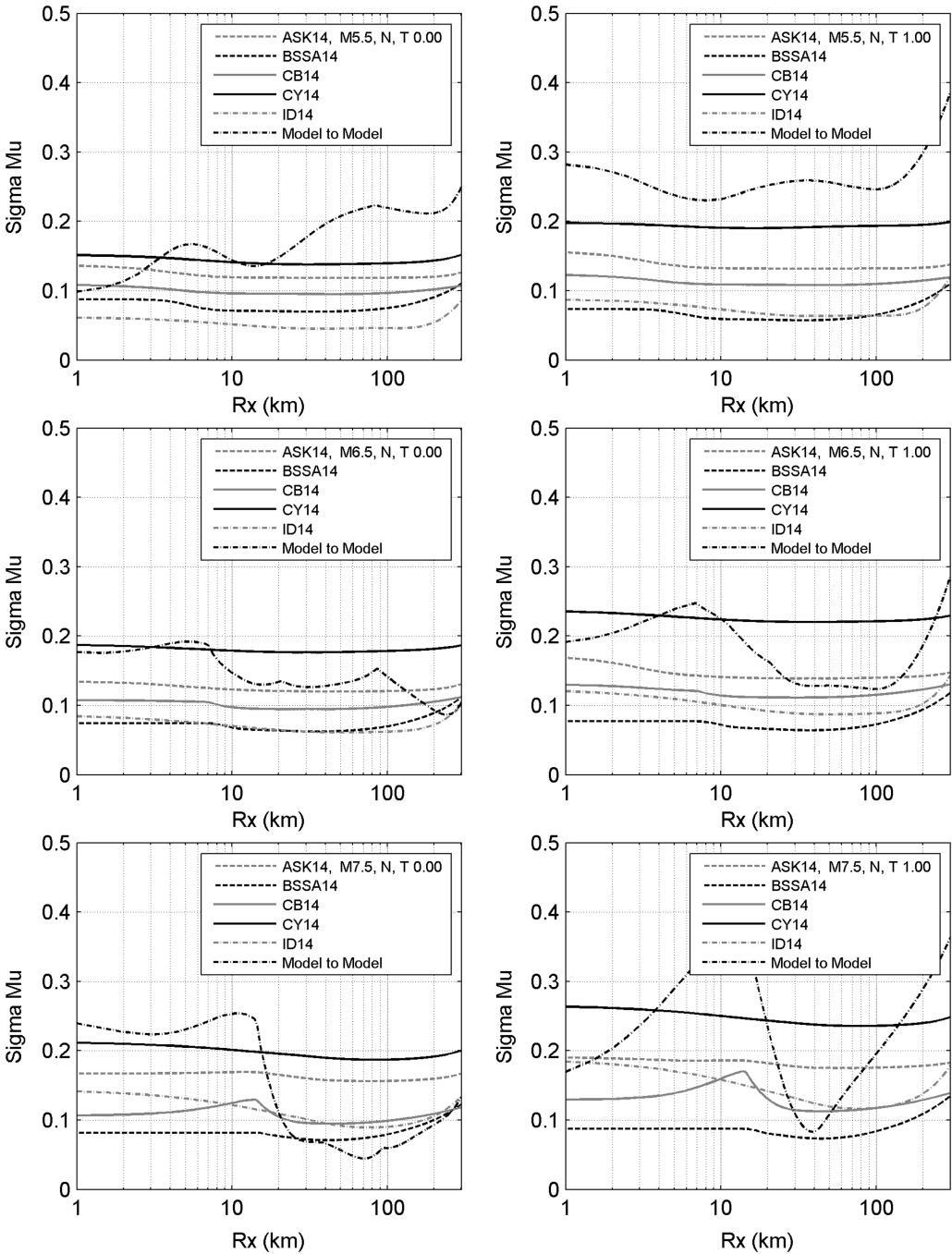


**Figure 4.** Asymptotic standard errors and model-to-model variability in median  $\ln(\text{PSA})$  for the five NGA-West2 models for the normal (N) rupture scenarios shown in Figure 1. Results are shown for PGA (left column) and 1.0 s PSA (right column) for  $M$  5.5 (top row),  $M$  6.5 (middle row), and  $M$  7.5 (bottom row) earthquakes.

## EPISTEMIC UNCERTAINTY MODEL

The goal of this study was to develop a simple model to represent the minimum epistemic uncertainty in median predictions for the individual NGA-West2 GMPEs, while capturing the main features of the uncertainty. A single model is proposed to be applied to all five GMPEs. In this section, we present an evaluation of the sensitivity of the within-model uncertainty of median predictions to different parameters such as dip angle, hanging wall/footwall, magnitude, distance, style of faulting (SOF), and spectral periods. Based on this evaluation, a simple model of the epistemic uncertainty of the median of NGA-West2 GMPEs is proposed.

### DIP ANGLE

The sensitivity of the within-model uncertainty in median predictions of the NGA-West2 models to the choice of dip angle is evaluated by estimating the asymptotic standard errors in median  $\ln(\text{PSA})$  for CB14 for the dipping rupture geometries shown in Figure 1 compared to the same rupture widths but with a dip angle of  $25^\circ$ . The results are shown on Figure 5. The difference in the median prediction uncertainty occurs mainly in the distance range of 10 km to 40 km, where sites lie over the hanging wall for the shallower dip but are beyond the hanging wall for the steeper dip. At other distances, fault dip has a small effect on the within-model uncertainty in the median predictions. Figure 6 shows the effect of fault dip angle on the model-to-model variability, which is much greater than the effect on within-model uncertainty. The model-to-model variability is therefore considered adequate in capturing the increase in uncertainty in median predictions for shallower dip angles.

### HANGING WALL/FOOTWALL

The sensitivity of the within-model uncertainty in median predictions of the NGA-West2 models to the site being located on the hanging wall side versus the footwall side of the fault rupture plane was evaluated by estimating the asymptotic standard errors in median  $\ln(\text{PSA})$  for CB14 for rupture geometries shown in Figure 1. These evaluations show that the within-model uncertainty on the hanging wall is slightly larger than that on the footwall and that the within-model uncertainty on the footwall is nearly distance-independent. Therefore, in building an epistemic uncertainty model, we only consider hanging wall scenarios and apply the same model for footwall scenarios.

### DISTANCE DEPENDENCE

The within-model uncertainty in median predictions is averaged over distance for all five NGA-West2 models for each magnitude, distance, and style of faulting scenario. The average within-model uncertainty in median predictions is shown in Figure 7 for the rupture scenarios in Figure 1 with  $M$  5.5 through  $M$  7.5 at PGA and 1.0 s PSA. The average within-model uncertainty in median predictions does not show strong distance dependence for strike-slip faulting. For reverse and normal faulting, and particularly for magnitudes greater than 6, a stronger distance dependence is observed, with the average within-model uncertainty in median predictions being larger at close distances.

Despite this observed distance dependence, the proposed epistemic uncertainty model is distance-independent. This is due to the fact that this distance dependence is generally captured in the model-to-model variability shown in Figures 2 through 4. In addition, a single

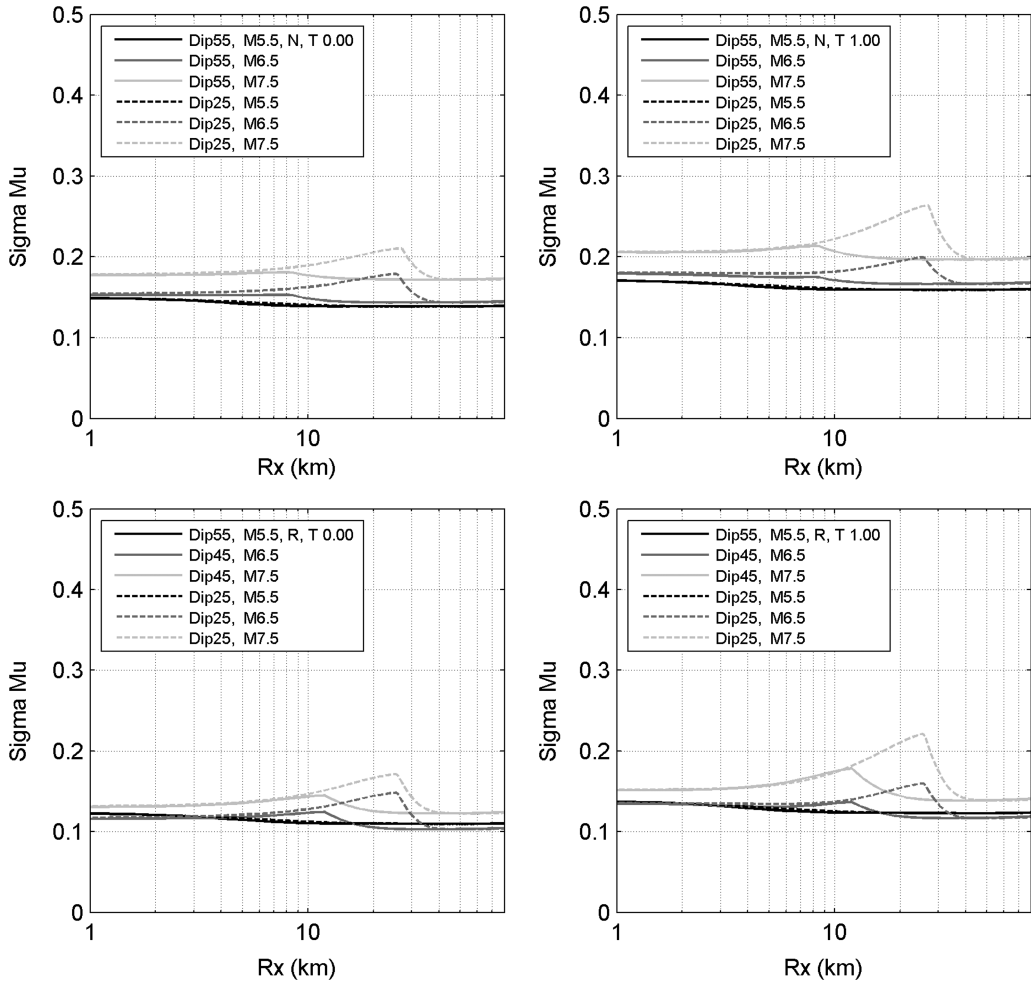


**Figure 5.** Comparison of asymptotic standard errors in median  $\ln(\text{PSA})$  for CB14 for the normal and reverse rupture scenarios in Figure 1 with different dip angles. Top row shows PGA (left) and 1 s PSA (right) for normal faulting. Bottom row shows PGA (left) and 1 s PSA (right) for reverse faulting.

epistemic uncertainty model is proposed for both hanging wall and footwall scenarios. For footwall scenarios, the within-model uncertainty is smaller and distance-independent.

## MAGNITUDE AND STYLE OF FAULTING

The within-model uncertainty in median predictions was averaged arithmetically over distances of 1 km to 200 km for each of the five NGA-West2 models. The upper limit of 200 km was chosen because it corresponds to the limit of applicability of most of the models. The resulting constant within-model uncertainties with distance were averaged

for all five NGA-West2 models. This leads to a single average within-model uncertainty in median predictions for all the GMPEs and at all distances for a given magnitude and style of faulting scenario. Figure 8 shows the average within-model uncertainty versus magnitude for the rupture geometries in Figure 1. The within-model uncertainty in median predictions is

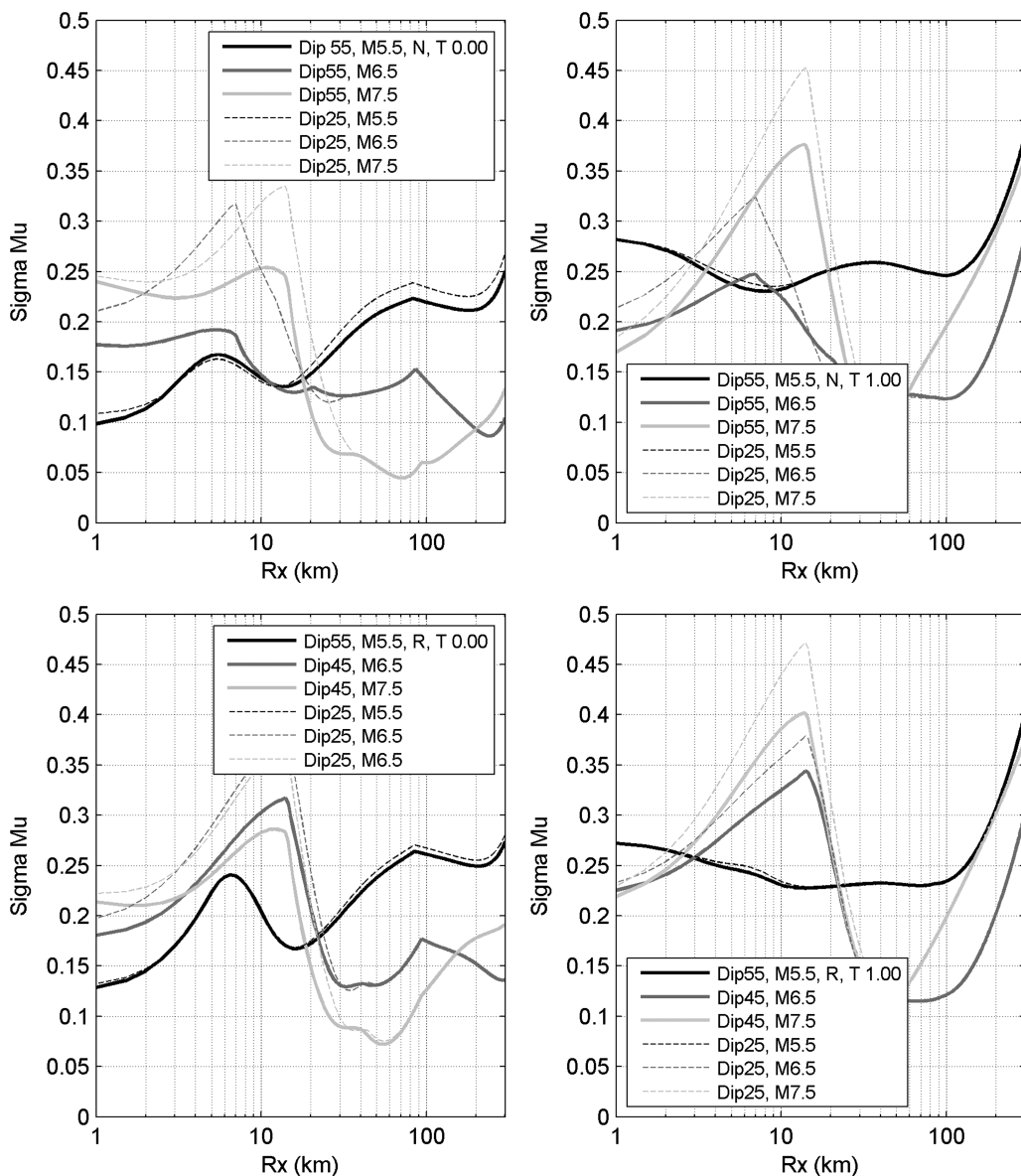


**Figure 6.** Comparison of model-to-model variability in median  $\ln(\text{PSA})$  of the five NGA-West2 GMPEs for the normal and reverse rupture scenarios in Figure 1 with different dip angles. Top row shows PGA (left) and 1 s PSA (right) for normal faulting. Bottom row shows PGA (left) and 1 s PSA (right) for reverse faulting.

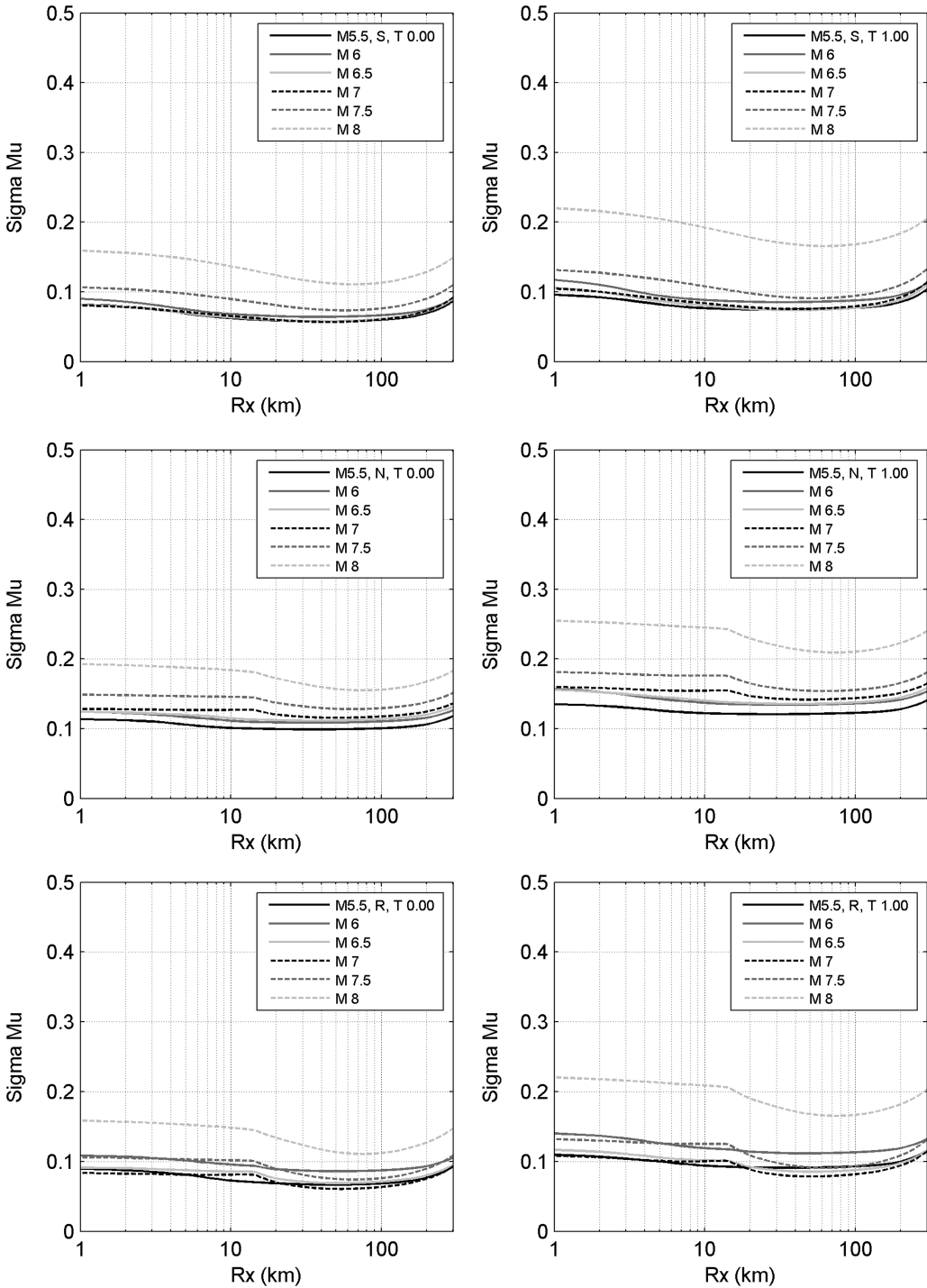


**Figure 7.** Average asymptotic standard errors in median  $\ln(\text{PSA})$  for the five NGA-West2 models for the rupture scenarios shown in Figure 1 at PGA (left) and 1.0 s PSA (right). Top row shows the results for strike-slip faulting, middle row for normal faulting and bottom row for reverse faulting.

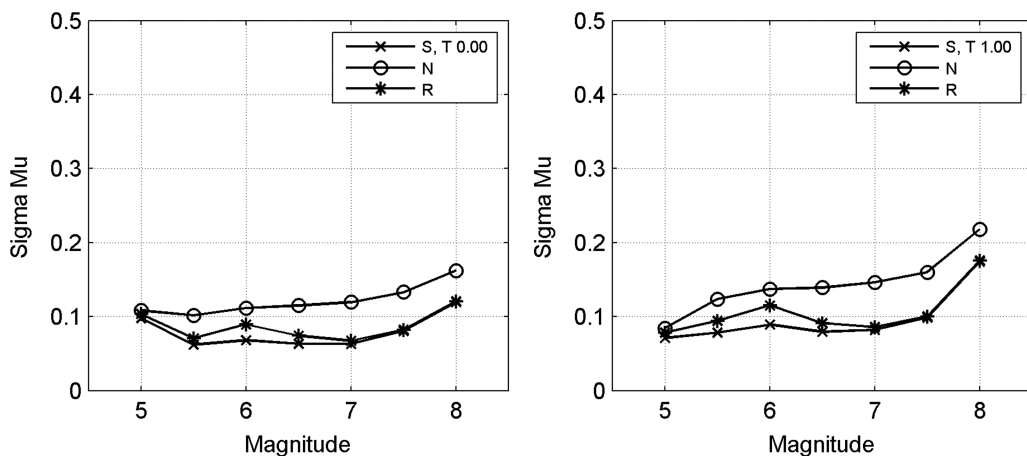


**Figure 8.** Average within-event uncertainty over distance and over NGA-West2 models versus magnitude for the rupture geometries in Figure 1 for PGA and 1.0 s PSA.

near constant for  $M$  5.5 to  $M$  7.0 and then increases for magnitudes greater than 7.0. Strike-slip and reverse faulting scenarios have generally similar within-model uncertainty in median predictions, and normal faulting scenarios exhibit larger uncertainty. Based on these observations, we propose an epistemic uncertainty model that is constant for  $M$  5.0 to  $M$  7.0 and then increases for magnitudes greater than 7.0. The proposed epistemic uncertainty model assigns the same level of uncertainty in median predictions to strike-slip and reverse faulting earthquake motions, and slightly larger uncertainty for normal faulting earthquake motions.

### SPECTRAL PERIOD DEPENDENCE

Figure 9 shows the average within-model uncertainty in median predictions versus spectral period for the five NGA-West2 models for the rupture geometries in Figure 1 for  $M$  5.5 through  $M$  8.0. These values represent the average over distances of 0 km to 200 km, as described in the previous section. The average within-model uncertainty for median predictions of the five NGA-West2 models can be approximated by a constant for periods less than 1.0 s. At longer periods, the within-model uncertainty increases.

### PROPOSED MODEL

Based on the evaluation of magnitude, distance, style of faulting, and spectral period dependence of the average within-model uncertainty in median predictions of the NGA-West2 models, a distance-independent epistemic uncertainty model of the median ground motion is proposed. For strike-slip and reverse faulting scenarios with magnitude 5.0 to 7.0, a constant epistemic standard deviation 0.083 natural log units is assigned for spectral periods less than 1.0 s. For larger magnitudes and longer periods, this uncertainty is increased, as shown in the equations below. For normal faulting scenarios, an additional 0.038 natural log units is added to the standard deviation for strike-slip and reverse faulting scenarios.

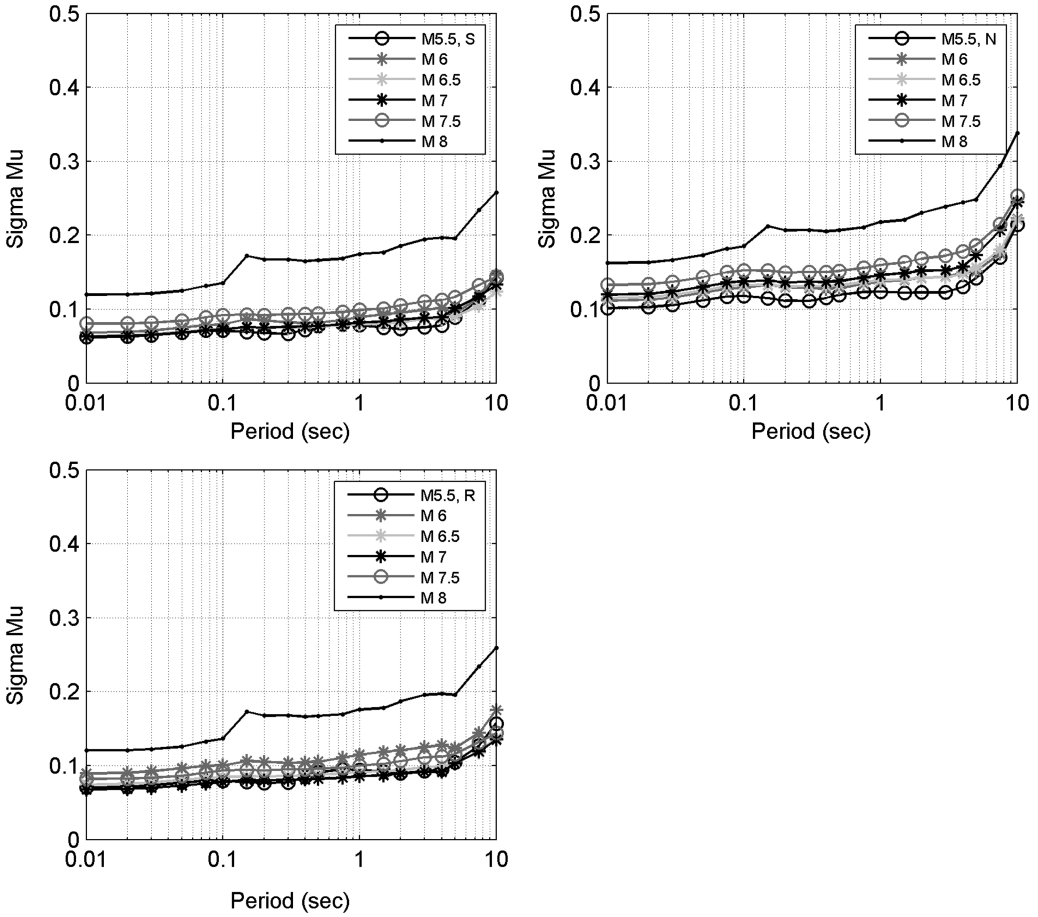


**Figure 9.** Average within-event uncertainty over distance and over NGA-West2 models versus spectral periods for the rupture geometries in Figure 1.

For strike-slip and reverse faulting:

- For spectral periods less than 1.0 s:

$$\sigma_{\mu \ln(psa)}(SS, RV, T < 1.0) = \begin{cases} 0.083 & \text{for } M < 7.0 \\ 0.056 * (M - 7.0) + 0.083 & \text{for } M \geq 7.0 \end{cases} \quad (9)$$

- For spectral periods greater than or equal to 1.0 s:

$$\sigma_{\mu \ln(psa)}(SS, RV, T \geq 1.0) = \sigma_{\mu \ln(psa)}(T < 1.0) + 0.0171 * \ln(T) \quad (10)$$

For normal faulting:

$$\sigma_{\mu \ln(psa)}(NM, T) = \sigma_{\mu \ln(psa)}(RV, T) + 0.038 \quad (11)$$

where  $M$  is the moment magnitude,  $T$  is the spectral period in seconds and  $SS$  and  $RV$  refer to strike-slip and reverse faulting scenarios, respectively.

This proposed uncertainty model captures the average uncertainty in median predictions of the NGA-West2 models except for conditions with very limited data on the hanging wall at close distance and for very shallow dip angles. The larger uncertainty for these particular cases is captured by the larger variability among the five NGA-West2 models. Therefore, the larger epistemic uncertainty for these locations is accounted for in the overall estimate.

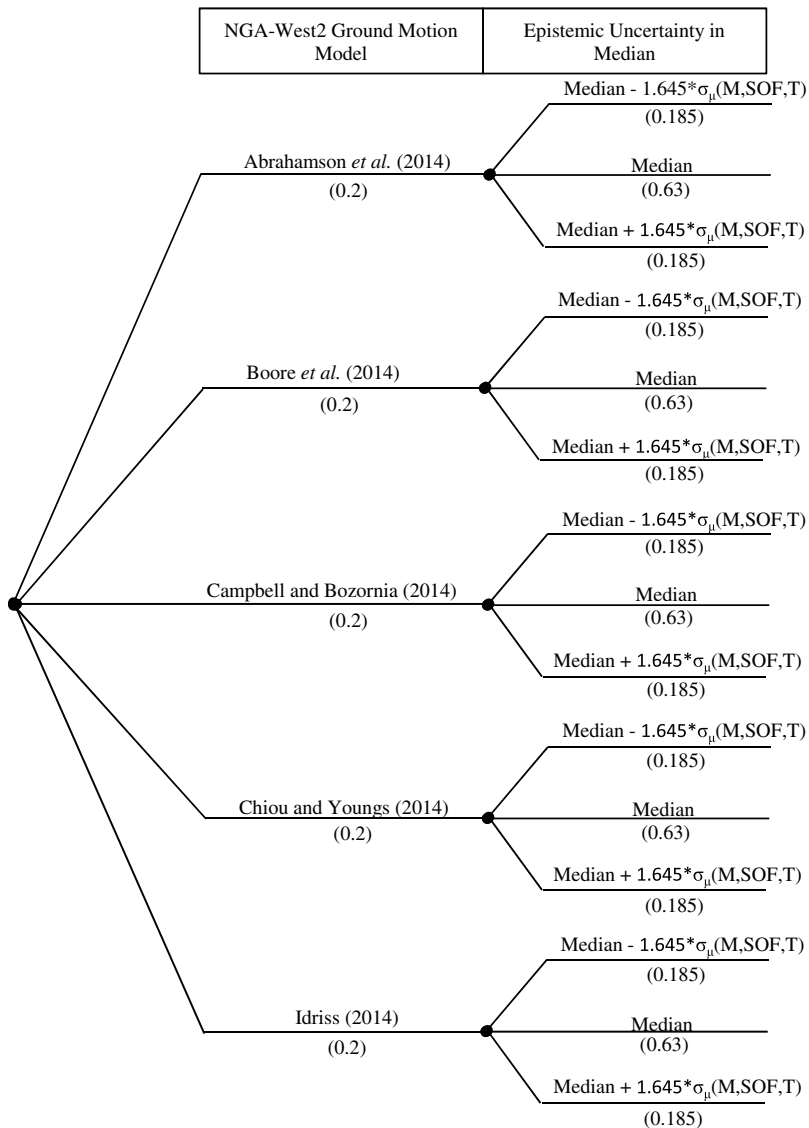


**Figure 10.** Proposed logic tree for NGA-West2 models. M refers to magnitude, SOF to style of faulting, and T to spectral period.

The epistemic uncertainty in the median prediction for an individual NGA-West2 GMPE is modeled using a three-point discrete approximation to a normal distribution (Keefer and Bodily 1983). This approach places a weight of 0.63 on the median model and weights of 0.185 on the 5th and the 95th percentiles ( $\pm 1.645$  standard deviations). This approach is implemented by developing three alternative models for each NGA-West2 GMPE: one model equal to the original GMPE median and two models with  $\pm 1.645\sigma_{\mu \ln(psa)}$  added to the median, each with weight 0.185. The resulting logic tree for crustal earthquake ground motion models is shown in Figure 10, assuming equal weight assigned to each of the five NGA-West2 GMPEs.

In the 2014 update of the USGS National Seismic Hazard Maps (NSHMs), Rezaeian et al. (2014) apply an updated version of the “square-root rule” epistemic uncertainty model developed by Petersen et al. (2008) to estimate the additional epistemic uncertainty to be assigned to the median prediction of the 4 NGA-West2 GMPEs (ASK14, BSSA14, CB14, and CY14). Their epistemic uncertainty is period-independent, but varies for different magnitude and distance bins. Table 2 compares the USGS epistemic uncertainty to the minimum epistemic uncertainty recommended in this study. The USGS values represent approximate 90% uncertainty intervals and were converted to equivalent standard deviations of  $\ln(\text{PSA})$  by dividing by 1.645. The USGS-adopted values are larger than the ones proposed herein, especially for scenarios at short distances. These differences are due to different approaches used. The USGS estimates are based on an assumed level of epistemic uncertainty for the large-magnitude–short-distance bin and then on assigning uncertainties to the other magnitude and distance bins based on the relative number of earthquakes contributing to each bin. As such, the assigned uncertainties would vary depending upon the specification of the magnitude-distance bins and the initial assessment for one of the bins. The uncertainties reported in this paper are based on direct statistical estimates of how well the data constrain the predictions of the individual NGA-West2 models and do not depend on specification of magnitude-distance bins. They are, however, considered to represent minimum epistemic uncertainties.

**Table 2.** Comparison of epistemic uncertainty used with the NGA-West2 models in the 2014 update of the NSHMs and the minimum epistemic uncertainty proposed in this study for strike-slip, reverse, and normal faults and spectral periods of up to 1 s

		USGS	This study SS, RV, T0 to T1 s	This study NM, T0 to T1 s
$5 \leq M < 6$	$R \leq 10$ km	0.225	0.083	0.121
	$10 \text{ km} \leq R \leq 30$ km	0.134	0.083	0.121
	$30 \leq R$	0.134	0.083	0.121
$6 \leq M < 7$	$R \leq 10$ km	0.152	0.083	0.121
	$10 \text{ km} \leq R \leq 30$ km	0.140	0.083	0.121
	$30 \text{ km} \leq R$	0.140	0.083	0.121
$7 \leq M$	$R \leq 10$ km	0.243	0.111 (M 7.5)	0.149 (M 7.5)
	$10 \text{ km} \leq R \leq 30$ km	0.219	0.111 (M 7.5)	0.149 (M 7.5)
	$30 \text{ km} \leq R$	0.201	0.111 (M 7.5)	0.149 (M 7.5)

## SUMMARY

We presented a simple model to assign additional epistemic uncertainty to the median predictions of each of the five NGA-West2 GMPEs in a logic tree framework. The epistemic uncertainty was evaluated based on the model-to-model differences and on the statistics of the model fits and empirical data distributions, while accounting for imposed model constraints. The proposed additional epistemic uncertainty is distance-independent, but it depends on magnitude, style of faulting, and spectral period. The five NGA-West2 models are given equal weights and the epistemic uncertainty in the median predictions is modeled using a three-point discrete approximation to a normal distribution. This additional epistemic uncertainty represents the minimum uncertainty to be used with the NGA-West2 models. It has been the experience of the second author that inclusion of additional epistemic uncertainty on the order of the model presented in this paper produces a small to moderate increase in computed seismic hazard compared to just utilizing the published NGA models equally weighted. The increase in mean annual frequency of exceedance typically ranges from a few percent at low ground motion levels to 20% to 25% at large ground motion levels.

## ACKNOWLEDGMENTS

This study was sponsored by the Pacific Earthquake Engineering Research Center (PEER) and was funded by the California Earthquake Authority, the California Department of Transportation, and the Pacific Gas & Electric Company. Any opinions, findings, and conclusions or recommendations expressed in this material are those of the authors and do not necessarily reflect those of the sponsoring agencies. We would like to thank the developers of the five NGA-West2 models for the insightful feedback during the development of the proposed epistemic uncertainty model.

## REFERENCES

- Abrahamson, N. A., and Youngs, R. R., 1992. A stable algorithm for regression analyses using the random effects model, *Bulletin of the Seismological Society of America* **82**, 505–510.
- Abrahamson, N. A., Silva, W. J., and Kamai, R., 2014. Summary of the ASK14 ground motion relation for active crustal regions, *Earthquake Spectra* **30**, 1025–1055.
- Abrahamson, N. A., Atkinson, G., Boore, D., Bozorgnia, Y., Campbell, K., Chiou, B. S.-J., Idriss, I. M., Silva, W., and Youngs, R. R., 2008. Comparisons of the NGA ground-motion relations, *Earthquake Spectra* **24**, 45–66.
- BC Hydro, Inc., 2012. *Probabilistic Seismic Hazard Analysis (PSHA) Model*, Volumes 1, 2, 3, and 4, Engineering Report E658, November 2012.
- Boore, D. M., Stewart, J. P., Seyhan, E., and Atkinson, G. A., 2014. NGA-West2 equations for predicting PGA, PGV, and 5% damped PSA for shallow crustal earthquakes, *Earthquake Spectra* **30**, 1057–1085.
- Campbell, K. W., and Bozorgnia, Y., 2014. NGA-West2 ground motion model for the average horizontal components of PGA, PGV, and 5% damped linear acceleration response spectra, *Earthquake Spectra* **30**, 1087–1115.
- Chiou, B. S.-J., and Youngs, R. R., 2008. An NGA model for the average horizontal component of peak ground motion and response spectra, *Earthquake Spectra* **24**, 173–215.

- Chiou, B. S.-J., and Youngs, R. R., 2014. Update of the Chiou and Youngs NGA model for the average horizontal component of peak ground motion and response spectra, *Earthquake Spectra* **30**, 1117–1153.
- Idriss, I. M., 2014. An NGA-West2 empirical model for estimating the horizontal spectral values generated by shallow crustal earthquakes, *Earthquake Spectra* **30**, 1155–1177.
- Keefer, D. L., and Bodily, S. E., 1983. Three-point approximations for continuous random variables, *Management Science* **29**, 595–609.
- Petersen, M. D., Frankel, A. D., Harmsen, S. C., Mueller, C. S., Haller, K. M., Wheeler, R. L., Wesson, R. L., Zeng, Y., Boyd, O. S., Perkins, D. M., Luco, N., Field, E. H., Wills, C. J., and Rukstales, K. S., 2008. *Documentation for the 2008 Update of the United States National Seismic Hazard Maps*, U.S. Geological Survey Open-File Report 2008-1128, Reston, VA.
- Rezaeian, S., Petersen, M. D., Moschetti, M. P., Powers, P., Harmsen, S. C., and Frankel, A. D., 2014. Implementation of NGA-West2 ground motion models in the 2014 U.S. National Seismic Hazard Maps, *Earthquake Spectra* **30**, 1319–1333.
- Searle, S. R., 1971. *Linear Models*, John Wiley & Sons, New York, 560 pp.
- Seber, G. A. F., and Wild, C. J., 1989. *Nonlinear Regression*, John Wiley & Sons, New York, 792 pp.
- U.S. Nuclear Regulatory Commission (USNRC), 2012. *Practical Implementation Guidelines for SSHAC Level 3 and 4 Hazard Studies*, NUREG 2117, Washington, D.C.

(Received 28 June 2013; accepted 22 March 2014)